JGP Journal of General Physiology

RESEARCH ARTICLE

Regulatory light chain phosphorylation augments length-dependent contraction in PTU-treated rats

Jason J. Breithaupt, Hannah C. Pulcastro, Peter O. Awinda, David C. DeWitt, and Bertrand C.W. Tanner

Force production by actin–myosin cross-bridges in cardiac muscle is regulated by thin-filament proteins and sarcomere length (SL) throughout the heartbeat. Prior work has shown that myosin regulatory light chain (RLC), which binds to the neck of myosin heavy chain, increases cardiac contractility when phosphorylated. We recently showed that cross-bridge kinetics slow with increasing SLs, and that RLC phosphorylation amplifies this effect, using skinned rat myocardial strips predominantly composed of the faster α-cardiac myosin heavy chain isoform. In the present study, to assess how RLC phosphorylation influences length-dependent myosin function as myosin motor speed varies, we used a propylthiouracil (PTU) diet to induce >95% expression of the slower β-myosin heavy chain isoform in rat cardiac ventricles. We measured the effect of RLC phosphorylation on Ca^{2+}-activated isometric contraction and myosin cross-bridge kinetics (via stochastic length perturbation analysis) in skinned rat papillary muscle strips at 1.9- and 2.2-µm SL. Maximum tension and Ca^{2+} sensitivity increased with SL, and RLC phosphorylation augmented this response at 2.2-µm SL. Subtle increases in viscoelastic myocardial stiffness occurred with RLC phosphorylation at 2.2-µm SL, but not at 1.9-µm SL, thereby suggesting that RLC phosphorylation increases β-myosin heavy chain binding or stiffness at longer SLs. The cross-bridge detachment rate slowed as SL increased, providing a potential mechanism for prolonged cross-bridge attachment to augment length-dependent activation of contraction at longer SLs. Length-dependent slowing of β-myosin heavy chain detachment rate was not affected by RLC phosphorylation. Together with our previous studies, these data suggest that both α- and β-myosin heavy chain isoforms show a length-dependent activation response and prolonged myosin attachment as SL increases in rat myocardial strips, and that RLC phosphorylation augments length-dependent activation at longer SLs. In comparing cardiac isoforms, however, we found that β-myosin heavy chain consistently showed greater length-dependent sensitivity than α-myosin heavy chain. Our work suggests that RLC phosphorylation is a vital contributor to the regulation of myocardial contractility in both cardiac myosin heavy chain isoforms.

Introduction

Actin–myosin cross-bridge interactions use energy from ATP hydrolysis to generate the contractile force in cardiac muscle, which enables the heart to pump blood throughout the body. Troponin, a regulatory protein on the thin filament, binds intracellular Ca^{2+} and interacts with tropomyosin to biochemically regulate these cross-bridge interactions. Structural changes that accompany variations in sarcomere length (SL) also modulate the degree of thick and thin filament overlap to influence the number of cross-bridges available to generate force throughout a heartbeat (Tobacman, 1996; Cooke, 1997). Myosin regulatory light chain (RLC) binds to the neck of myosin, and posttranslational phosphorylation of RLC is thought to augment force production by increasing cross-bridge recruitment to the force-generating population (Morano et al., 1985; Sweeney and Stull, 1986, 1990; Sweeney et al., 1993; Olsson et al., 2004; Stelzer et al., 2006; Colson et al., 2010).

Recent observations from our laboratory suggest that cross-bridge cycling kinetics slow with increases in SL related to a reduced rate of magnesium adenosine diphosphate dissociation from cross-bridges (Tanner et al., 2015). We also found that RLC phosphorylation decreases the magnesium adenosine triphosphate binding rate, making cross-bridge detachment occur more slowly (Pulcastro et al., 2016). This finding was consistent with previous studies suggesting that RLC phosphorylation slows cross-bridge detachment (Franks et al., 1984; Patel et al., 1998; Olsson et al., 2004; Stelzer et al., 2006; Greenberg et al., 2009;

Department of Integrative Physiology and Neuroscience, Washington State University, Pullman, WA.

Correspondence to Bertrand C.W. Tanner: bertrand.tanner@wsu.edu.

This work is part of a special collection on myofilament function.

Colson et al., 2010), although other groups have proposed that RLC phosphorylation repositions myosin heads nearer to thin filaments, to facilitate cross-bridge recruitment (Sweeney and Stull, 1990; Levine et al., 1998; Stelzer et al., 2006; Colson et al., 2010).

Contractility of the cardiac atria and ventricles is modulated by various percentages of α- and β-cardiac myosin heavy chain, depending on the species and health of the heart (Lompré et al., 1984; Reiser and Kline, 1998; Reiser et al., 2001). Previously, our laboratory used skinned myocardial strips from the left ventricle of rats to assess the individual and combined effects of RLC phosphorylation and SL on myosin kinetics, the isometric force–free calcium concentration (pCa = $-\log[Ca^{2+}]$) relationship, and viscoelastic myocardial stiffness (Tanner et al., 2015; Pulcastro et al., 2016). These myocardial strips predominantly expressed the faster cardiac myosin heavy chain isoform (α-cardiac; *Myh6* gene). Thus, we sought to assess how RLC phosphorylation influences length-dependent myosin function and cardiac contractility as myosin motor speed varies, by using myocardial strips expressing the slower cardiac myosin heavy chain isoform (β-cardiac; *Myh7* gene). We hypothesized that the effects of RLC phosphorylation on cross-bridge function would be amplified at longer SLs because of slower cross-bridge cycling rates in myocardial strips expressing primarily β-myosin heavy chain. To test this hypothesis, we fed rats 6-*n*-propyl-2-thiouracil (PTU) to induce >95% expression of the slower β-myosin heavy chain isoform in the cardiac ventricles. We then measured tension–pCa relationships and myosin cross-bridge kinetics, as RLC phosphorylation varied at short and long SLs in skinned papillary muscle strips from these rats. We found that RLC phosphorylation increased both Ca^{2+} sensitivity of the tension–pCa relationship and maximal tension development of the tension–pCa relationship at 2.2-µm SL, but not at 1.9-µm SL. Thus, RLC phosphorylation may enhance cardiac contractility only at longer SLs in myocardial tissue expressing predominantly the β-myosin heavy chain isoform. We also found that the β-myosin heavy chain cross-bridge detachment rate slows under maximally activated conditions (pCa 4.8) at the longer 2.2-µm SL. We observed a more significant length-dependent effect in this current study in myocardial strips predominantly composed of β-myosin heavy chain, versus the length-dependent effects seen in our previous study of strips primarily composed of α-myosin heavy chain. These findings may represent molecular mechanisms to accommodate increased contractile demand at longer SL caused by increased diastolic filling in regions of the heart expressing predominantly β-myosin heavy chain, such as the human cardiac ventricles (Hamilton and Ianuzzo, 1991).

Materials and methods

Animal models

All procedures were approved by the Institutional Animal Care and Use Committee at Washington State University and complied with the *Guide for the Use and Care of Laboratory Animals* published by the National Institutes of Health. Adult male Sprague-Dawley rats were acquired from Simonsen Laboratories and fed an iodine-deficient 0.15% PTU chow (Harlan Teklad) for 10 wk, at which point they were euthanized ($n = 8$, age 16–20 wk).

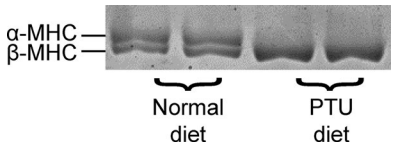

Figure 1. **Effect of PTU on cardiac myosin heavy chain expression.** Gel electrophoresis of left ventricle tissue homogenate stained with Coomassie blue shows the predominant shift toward β-myosin heavy chain expression in PTU-fed rats. MHC, myosin heavy chain.

This diet shifts the myosin isoform expression profile from predominantly α-myosin heavy chain to β-myosin heavy chain in rodents (Pope et al., 1980; Fitzsimons et al., 1998; Palmer et al., 2007; Ford and Chandra, 2013; Wang et al., 2013). Expression of many myofilament regulatory proteins has been shown to be unaffected by hypothyroidism, including troponin T, I, and C; myosin light chain I (essential light chain) and II (RLC); actin; and α-tropomyosin (Fitzsimons et al., 1998; Ford and Chandra, 2013). Rats were anesthetized by isoflurane inhalation (3% volume in 95% O_2-5% CO_2 flowing at 2 liters/min), and hearts were immediately excised and placed in dissecting solution on ice.

Biochemical quantification of myosin isoform content

Myosin isoform expression was measured via gel electrophoresis, as previously described (Reiser and Kline, 1998). Left ventricle samples were taken from (a) sex- and age-matched control rat hearts that were fed a standard laboratory diet (5001; LabDiet) and (b) each PTU-treated rat heart. The samples were run in duplicate, and gels were stained with Coomassie Brilliant blue (Thermo Fisher Scientific) and scanned on a Perfection v750 Pro (Epson). The relative optical densities of α-myosin heavy chain to β-myosin heavy chain isoform were quantified with ImageJ (National Institutes of Health). Among all PTU-treated rat cardiac samples, β-myosin heavy chain content was >95% (Fig. 1).

Solutions for skinned myocardial strips

Muscle mechanics solution concentrations were formulated by solving equations describing ionic equilibria according to Godt and Lindley (1982), and all concentrations are listed in millimolar, unless otherwise noted. Dissecting solution: 50 N,N-Bis(2-hydroxyethyl)taurine, 30.83 potassium-propionate, 10 Na-azide, 20 EGTA, 6.29 $MgCl_2$, 6.09 ATP, 1 dithiothreitol, 20 2,3-butanedione monoxime, 50 µM leupeptin, 275 µM Pefabloc (Acros Organics), and 1 µM E-64. Skinning solution: dissecting solution with 1% Triton-X-100 (wt/vol) and 50% glycerol (wt/vol). Storage solution: dissecting solution and 50% glycerol (wt/vol). Relaxing solution: pCa 8.0, 5 EGTA, 5 MgATP, 1 Mg^{2+}, 0.3 P_i, 35 phosphocreatine, and 300 U/ml creatine kinase, 200 ionic strength (pH 7.0). Activating solution: same as relaxing solution with pCa 4.8. Alkaline phosphatase (AP) solution: same as relaxing solution with 6 U/ml recombinant AP from *Escherichia coli*. Myosin light chain kinase (MLCK) solution: same as relaxing with pCa 6.0, 1.1 µM human skeletal MLCK, and 12 µM *Xenopus* calmodulin.

Skinned myocardial strips

Left ventricular papillary muscles were dissected from each heart and pared down to thin strips (500–700 µm long and 150–200 µm

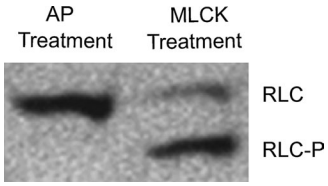

Figure 2. **In vitro RLC phosphorylation of skinned papillary muscle strips.** Western blot after 1-d isoelectric gel electrophoresis shows the typical ratios of nonphosphorylated RLC and phosphorylated RLC (RLC-P) in skinned papillary muscle strips that were used for mechanics measurements. AP-treated strips showed no detectible RLC-P, whereas MLCK-treated strips showed ∼68% RLC-P.

wide at their minor and major axes, forming an ellipse). Strips were skinned overnight at 4°C and stored at −20°C for up to 1 wk. Aluminum T-clips were attached to the end of each strip, and the strips were mounted between a piezoelectric motor (P841.40; Physik Instrumente) and a strain gauge (AE801; Kronex), lowered into a 30-µl droplet of relaxing solution maintained at 17°C, and stretched to 1.9- or 2.2-µm SL measured by digital Fourier transform (IonOptix Corp.). We had previously investigated whether some cardiac effects of hypothyroidism may be partially related to changes in myofilament protein phosphorylation, specifically a decrease in Ca^{2+} sensitivity of contraction caused by increased troponin I phosphorylation. However, we found that AP treatment of skinned myocardial strips removed any of these effects (Wang et al., 2013). Consequently, we applied a similar AP pretreatment to our strips to produce a homogeneous phosphorylation profile among all experiments, and we did not observe any significant differences between PTU strips (herein) and non-PTU strips (Pulcastro et al., 2016).

All strips were pretreated in AP solution at room temperature for 10 min and mounted on the experimental apparatus in relaxing solution (pCa 8.0). After AP pretreatment, one group of strips was calcium activated from pCa 8.0 to pCa 4.8; there was no detectable RLC phosphorylation in these AP-treated strips. Another group of strips underwent the AP pretreatment, after which the strips were incubated in MLCK solution for 30 min, and then these strips received the identical Ca^{2+}-activation protocol as the AP-treated strips. The mean percentage of RLC phosphorylation was 67.8 ± 5.5% in MLCK-treated strips (Fig. 2; quantified with ImageJ [National Institutes of Health] as described by Pulcastro et al. [2016]). At least two strips from each of the eight hearts underwent the mechanics protocol for each condition, with the total number of strips for each condition listed in Table 1.

Table 1. **Values from the four-parameter Hill fits to tension–pCa relationships at 1.9- and 2.2-µm SLs**

Parameter	1.9 µm		2.2 µm	
	AP	MLCK	AP	MLCK
T_{min} (kN · m^{-2})	0.39 ± 0.09	0.39 ± 0.07	3.08 ± 0.40[a]	2.73 ± 0.32[a]
T_{max} (kN · m^{-2})	23.88 ± 0.90	23.36 ± 1.28	30.50 ± 2.09[a]	34.37 ± 2.05[a]
pCa_{50}	5.48 ± 0.02	5.49 ± 0.03	5.51 ± 0.02	5.57 ± 0.03[a]
n_H	7.3 ± 0.2	7.1 ± 0.3	6.5 ± 0.4[a]	6.4 ± 0.3
n strips	20	18	16	16

Data are means ± SEM. T_{min}, T_{max}, pCa_{50}, and n_H represent fit parameters to a four-parameter Hill equation for the absolute tension versus pCa relationship: $T(pCa) = (T_{max}/[1 + 10^{n_H(pCa-pCa_{50})}]) + T_{min}$.
[a]P < 0.05, effect of SL within the AP- or MLCK-treated group.

Dynamic mechanical analysis

Stochastic length perturbations were applied for a period of 60 s, as previously described (Tanner et al., 2011, 2015), by using an amplitude distribution with an SD of 0.05% muscle lengths over the frequency range 0.125–100 Hz. Elastic and viscous moduli, $E(\omega)$ and $V(\omega)$, were measured as a function of angular frequency (ω) from the in-phase and out-of-phase portions of the tension response to the stochastic length perturbation. Viscoelastic myocardial stiffness is represented by the complex modulus $Y(\omega) = E(\omega) + iV(\omega)$, where $i = \sqrt{-1}$. Fitting Eq. 1 to the entire frequency range of moduli values provided estimates of six model parameters (A, k, B, $2\pi b$, C, and $2\pi c$).

$$Y(\omega) = A(i\omega)^k - B\left(\frac{i\omega}{2\pi b + i\omega}\right) + C\left(\frac{i\omega}{2\pi c + i\omega}\right). \quad (1)$$

The A-term in Eq. 1 reflects the viscoelastic mechanical response of passive, structural elements in the muscle and holds no enzymatic dependence. The parameter A represents the combined mechanical stress of the strip, and the parameter k describes the viscoelasticity of these passive elements, where $k = 0$ represents a purely elastic response and $k = 1$ is a purely viscous response (Mulieri et al., 2002; Palmer et al., 2013). The B- and C-terms reflect enzymatic cross-bridge cycling behavior that produce frequency-dependent shifts in the viscoelastic mechanical response during Ca^{2+}-activated contraction. These B- and C-processes characterize work-producing (cross-bridge recruitment) and work-absorbing (cross-bridge detachment) muscle responses, respectively (Kawai and Halvorson, 1991; Campbell et al., 2004; Palmer et al., 2007). The parameters B and C represent the mechanical stress from the cross-bridges (i.e., number of cross-bridges formed × their mean stiffness), and the rate parameters $2\pi b$ and $2\pi c$ reflect cross-bridge kinetics that are sensitive to biochemical perturbations affecting enzymatic activity. Molecular processes contributing to recruitment and force generation underlie the cross-bridge recruitment rate, $2\pi b$. Similarly, processes contributing to cross-bridge detachment or force decay underlie the cross-bridge detachment rate, $2\pi c$.

Statistical analysis

All values are shown as mean ± SEM. Constrained nonlinear least squares fitting of Eq. 1 to complex moduli values was performed with sequential quadratic programming methods in Matlab (Mathworks). Statistical tests were performed with SPSS (IBM Statistics), using linear mixed models with pCa or frequency as a repeated measure for data shown in Figs. 3, 4, and 5, using main effects of MLCK treatment or SL, followed by a least significant difference post hoc comparison of the means. Linear mixed models were also applied to the parameter values for the four-param-

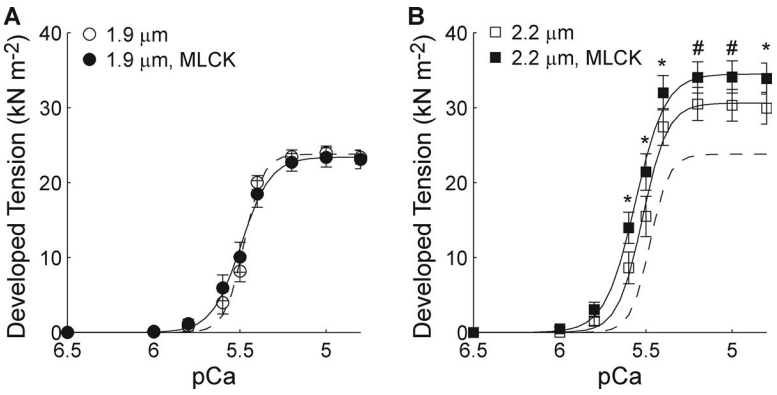

Figure 3. **RLC phosphorylation affected the tension–pCa relationship more at longer SLs. (A and B)** Developed tension–pCa relationships at 1.9-µm (A) and 2.2-µm (B) SLs for AP-treated and MLCK-treated skinned papillary muscle strips. Solid lines represent Hill fits to the tension–pCa data, with the dashed line representing the Hill fit of AP treated at 1.9-µm SL (replotted in B). *, P < 0.05; #, P < 0.1 between AP- and MLCK-treated conditions within each panel.

eter Hill fits to the tension–pCa relationships (Table 1) and fits to Eq. 1 (see Fig. 6).

Results

Isometric tension–pCa relationships

Isometric tension developed in a sigmoidal manner as skinned rat papillary muscle strips were Ca^{2+}-activated from pCa 8.0 to 4.8 (Fig. 3). These tension–pCa relationships were fitted to a four-parameter Hill equation (Table 1). As SL increased from 1.9 to 2.2 µm, Ca^{2+}-activated tension increased and became more sensitive to [Ca^{2+}] for both AP- and MLCK-treated strips ($P < 0.001$ for main effects of pCa, SL, and the pCa × SL interaction). MLCK treatment also increased tension development and Ca^{2+} sensitivity of the tension–pCa relationship, but only at the longer (2.2-µm) SL ($P = 0.017$ for the pCa × MLCK interaction). Ca^{2+}-activated tension increased more because of increased SL than increased RLC phosphorylation upon MLCK treatment. Increasing SL also led to robust increases in passive tension under relaxed conditions (pCa 8.0), without any significant effects of MLCK on passive tension (Table 1). These data show that the effect of RLC phosphorylation on Ca^{2+}-activated force development in myocardial strips becomes more pronounced as SL increases.

Myocardial viscoelasticity under relaxed conditions

Under relaxed conditions, myocardial viscoelasticity increased as SL increased from 1.9 to 2.2 µm, but there was no statistically significant effect of MLCK treatment at either SL (Fig. 4). Elastic moduli values were greater in 2.2- versus 1.9-µm SL strips for both AP- and MLCK-treated conditions at all frequencies >0.5 Hz (Fig. 4 A; $P < 0.001$ for main effects of frequency and SL). Viscous moduli values were also greater for 2.2- versus 1.9-µm SL (Fig. 4 B; $P = 0.014$ for main effect of frequency, $P < 0.001$ for main effect of SL), but these viscous moduli differences were not as large as the elastic moduli differences. These data also suggest that the length-dependent increases in viscoelastic myocardial stiffness arise from passive elements of the sarcomere (i.e., titin and collagen; Granzier and Irving, 1995), being stretched or extended more at 2.2-µm SL than at 1.9-µm SL. Their study suggests that titin dominates the passive response toward the shorter end of the working range for cardiac sarcomeres (SL ~1.9–2.2 µm), whereas collagen dominates at longer lengths (≥2.15 µm).

Myocardial viscoelasticity under Ca^{2+}-activated conditions

Both SL and MLCK treatment influenced the magnitude and frequency dependence of myocardial viscoelasticity near half-maximal activation (pCa 5.5) and at maximal calcium activation (pCa 4.8), shown in Fig. 5. We will initially focus on the effects of pCa level and SL within AP- and MLCK-treated strips and then will describe the effect of RLC phosphorylation. Comparing moduli responses within a panel illustrates the effect of submaximal versus maximal Ca^{2+} activation. For both SLs, the elastic (Fig. 5, A and B) and viscous (Fig. 5, C and D) moduli values were greater at pCa 4.8 versus 5.5, as expected because of greater cross-bridge binding and tension development at pCa 4.8. As SL increased

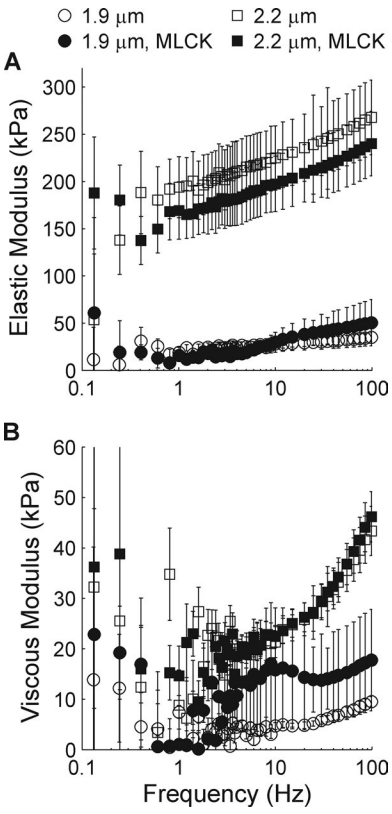

Figure 4. **RLC phosphorylation did not influence myocardial viscoelasticity under relaxed conditions. (A and B)** Elastic (A) and viscous (B) moduli were plotted against frequency at 1.9- and 2.2-µm SLs for AP- and MLCK-treated papillary muscle strips under relaxed conditions (pCa 8).

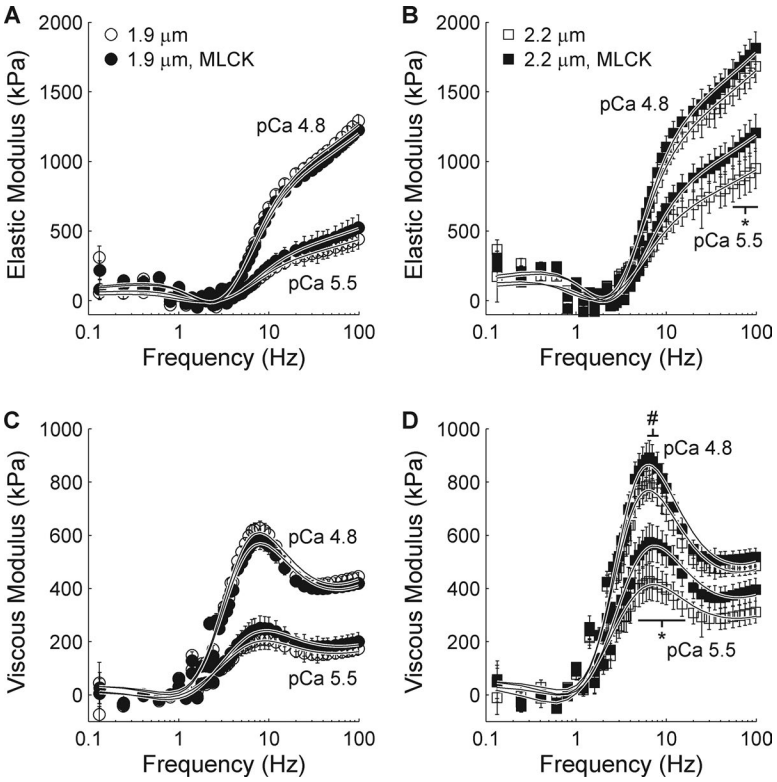

Figure 5. **RLC phosphorylation influenced myocardial viscoelasticity under Ca^{2+}-activated conditions at longer SLs. (A and B)** Elastic moduli were plotted against frequency at 1.9-μm (A) and 2.2-μm (B) SLs for AP- and MLCK-treated skinned papillary muscle strips under maximally activated conditions (pCa 4.8) and submaximally activated conditions near half-maximal tension (pCa 5.5). **(C and D)** The associated viscous moduli were plotted against frequency at 1.9-μm (C) and 2.2-μm (D) SLs. Lines represent fits to Eq. 1 for the complex moduli versus frequency relationships. Because frequency varied at either pCa 4.8 or 5.5, moduli values differed between AP- and MLCK-treated conditions at 2.2 μm SL. *, $P < 0.05$; #, $P < 0.1$.

from 1.9 to 2.2 μm, the magnitude of the elastic and viscous moduli values increased for AP- and MLCK-treated strips at both pCa levels ($P < 0.001$ for main effects of frequency, SL, and the frequency × SL interaction at both pCa 4.8 and 5.5). These data show robust increases in the elastic and viscous moduli values as Ca^{2+} activation and SL increased, whereas the effects of RLC phosphorylation caused by MLCK treatment were more subtle.

MLCK treatment did not affect myocardial viscoelasticity at 1.9-μm SL at either pCa level (Fig. 5, A and C). Under maximal Ca^{2+}-activated conditions (pCa 4.8) at 2.2-μm SL, MLCK treatment did not affect elastic moduli values and only modestly increased viscous moduli values between the frequencies of 6 and 8 Hz (Fig. 5 D; $P = 0.05$ for main effect of MLCK treatment, $P < 0.001$ for the frequency × MLCK interaction). At submaximal activation (pCa 5.5) and 2.2-μm SL, MLCK treatment increased elastic moduli values >55 Hz and viscous moduli between 5 and 14 Hz (Fig. 5, B and D, respectively; $P < 0.001$ for main effect of MLCK treatment). Shifts in the magnitude and frequency characteristics of this viscoelastic system response under Ca^{2+}-activated conditions reflect differences in cross-bridge cycling behavior. Typically, these kinetic parameters are reflected by the relative dips and peaks of the raw elastic and viscous modulus values at the lower to mid-frequency cycles, whereas the elastic modulus values continue to increase with frequency because of faster oscillations that sample a more "static" system where bridges appear to remain bound throughout a cycle period (Palmer et al., 2007, 2013; Palmer, 2010). Altogether, these moduli data show that the relative effects of RLC phosphorylation related to MLCK treatment were greatest at 2.2-μm SL and largely consistent between maximal and submaximal Ca^{2+} activation levels.

Moduli values were fitted to Eq. 1 to extract model parameters related to myocardial viscoelasticity, cross-bridge binding, and cross-bridge kinetics under maximally activated (pCa 4.8) and submaximally activated (pCa 5.5) conditions as SL and RLC phosphorylation varied (Fig. 6). At both levels of Ca^{2+} activation, *A* values increased at longer SL in AP- and MLCK-treated strips (Fig. 6 A). For both Ca^{2+} activation levels, *k* values also decreased at longer SL in AP-treated strips (Fig. 6 B). In combination, these increases in *A* and decreases in *k* indicate a more elastic characteristic of the myocardium at longer SL, which primarily arises from nonenzymatic (passive) characteristics of the tissue.

For both Ca^{2+} activation levels, *B* and *C* values increased at longer SL for MLCK-treated strips (Fig. 6, C and E). This suggests greater cross-bridge binding with RLC phosphorylation at 2.2-μm SL, providing a molecular mechanism that underlies the phosphorylation-dependent increases in tension observed at longer SL (Fig. 3 B). SL and MLCK treatment did not show a statistically significant effect on cross-bridge recruitment rate (Fig. 6 D, $2\pi b$), nor were there any consistent changes in recruitment rates between the two calcium activation levels in the entire set of measurements. However, the cross-bridge detachment rate ($2\pi c$) slowed as SL increased under maximally activated conditions, with and without RLC phosphorylation (Fig. 6 F), which could prolong the myosin duty ratio and contribute to greater cross-bridge binding upon RLC phosphorylation at 2.2-μm SL. There was a subtle increase in cross-bridge detachment rate as calcium activation decreased from pCa 4.8 to 5.5, but this change was only statistically significant for the rates at 2.2-μm SL (~30% faster ± RLC phosphorylation; $P < 0.05$). Again, these data suggest that the molecular effects of RLC phosphorylation

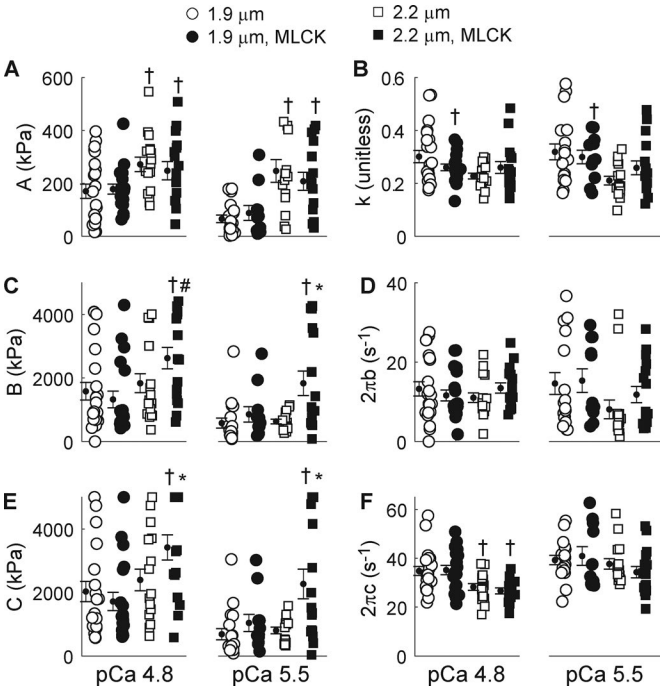

Figure 6. **RLC phosphorylation influenced myocardial viscoelasticity and cross-bridge behavior at pCa 4.8 and 5.5.** Parameter values from fits to Eq. 1 are shown for AP-and MLCK-treated strips as SL and Ca^{2+} activation varied. **(A and B)** Myocardial viscoelastic stiffness increased and became increasingly elastic as SL increased at pCa 4.8 and 5.5, reflected by the length-dependent increase in *A* values (A) and decrease in *k* values (B). **(C and E)** Magnitude parameters for the B processes (C) and C processes (E) increased with RLC phosphorylation at 2.2-μm SL for both Ca^{2+} activation levels. **(D and F)** The rate of cross-bridge recruitment, $2\pi b$ (D), was similar among all conditions, but the rate of cross-bridge detachment, $2\pi c$ (F), slowed at 2.2-μm SL at maximal Ca^{2+} activation (pCa 4.8). *, $P < 0.05$; #, $P < 0.1$ for an MLCK effect at the same SL; †, $P < 0.05$ for an SL effect within a group of AP- or MLCK-treated strips. Means ± SEM of each dataset are shown as the dot ± error bar just to the left of each scatter plot, within a panel.

that augment cross-bridge binding and force production become greater as SL increases.

Discussion

Effects of RLC phosphorylation of β-myosin heavy chain isoform are SL dependent

In this study, we performed biophysical muscle mechanics measurements to assess the influences of RLC phosphorylation and SL on the tension–pCa relationship and cross-bridge cycling kinetics in skinned rat papillary muscle strips that predominantly expressed the slower, cardiac β-myosin heavy chain isoform. RLC phosphorylation increased maximal isometric tension, calcium sensitivity of the tension–pCa relationship, and viscoelastic myocardial stiffness at submaximal calcium activation, but only at long SL (2.2 μm). These results suggest that RLC phosphorylation augments the number of bound cross-bridges and/or stiffness of force-generating cross-bridges, but this effect is more prominent at long SLs in myocardium containing β-myosin heavy chain. Cross-bridge detachment rate slowed as SL increased under maximally activated conditions. This slowed detachment rate could result in prolonged cross-bridge binding at longer SLs, which may contribute to greater contractility during systole in response to greater end-diastolic filling volumes. Collectively, these findings suggest that in myocardium predominantly expressing the β-myosin heavy chain isoform, the effects of RLC phosphorylation on tension development are codependent on SL. This study further indicates that RLC phosphorylation plays an important role in regulating myosin contributions to length-dependent activation of contraction.

The decrease in cross-bridge detachment rate at longer SLs ($2\pi c$, Fig. 6), with and without RLC phosphorylation, is associated with a longer duty ratio leading to increased viscoelastic myocardial stiffness as SL increased (Fig. 5). The relative shifts in viscoelastic myocardial stiffness that depend on RLC phosphorylation were smaller than the associated SL dependence. Moreover, the RLC-dependent increases in active viscoelasticity did not accompany frequency-dependent shifts in $2\pi b$ or $2\pi c$, even though the viscoelastic changes in RLC phosphorylation drove significant changes in *B* and *C* parameter values that represent cross-bridge binding. Overall, SL-dependent increases in cross-bridge binding and tension show the dominant effect. Any RLC phosphorylation–dependent increases in cross-bridge stiffness are not readily observed at shorter SLs and may be diminished by lower tension values and fewer cross-bridges binding at 1.9-μm SL. Therefore, the differences in active viscoelasticity related to RLC phosphorylation become more apparent at the longer SL because the effect of RLC phosphorylation on cross-bridge stiffness may be subtle, and increased cross-bridge recruitment dominates.

Relationship to our prior studies using myocardial strips expressing α-myosin heavy chain

Our previous study (Pulcastro et al., 2016) showed that RLC phosphorylation increased Ca^{2+}-sensitivity of contraction and maximal tension development at both 1.9- and 2.2-μm SL in MLCK-treated myocardial strips that primarily contained the faster cardiac α-myosin heavy chain isoform. In the current study, we observed a more robust length-dependent effect of tension development in β-myosin heavy chain isoform than in our prior study, with RLC phosphorylation augmenting length-dependent activation of contraction only at the longer SL (Fig. 3), which suggests that RLC phosphorylation increases cross-bridge binding for β-myosin heavy chain at long SLs, but not at short SLs. RLC phosphorylation of α-myosin heavy chain increased cross-bridge binding to augment Ca^{2+} sensitivity of the tension–pCa relationship at both SLs. It is noteworthy that tension values were similar in phosphorylated and dephosphorylated strips at submaximal Ca^{2+} concentrations in both β- and α-myosin heavy chain isoforms (Fig. 3 and Pulcastro et al., 2016). Thus, it is unlikely that there were significant differences in the population of cross-bridges bound for either myosin heavy chain isoform between these two studies. However, in combination, these studies suggest that β-myosin heavy chain is more sensitive to changes in SL, and the effects of RLC phosphorylation become amplified as SL increases for the β-myosin heavy chain isoform. Perhaps, with α-myosin heavy chain being less sensitive to changes in SL, the relative effects of RLC phosphorylation (vs. SL) influence

α-myosin heavy chain cross-bridge activity more greatly over a broader range of SL values.

In addition to these effects of RLC phosphorylation on tension development, we observed that increasing SL slowed cross-bridge detachment rate at maximum Ca^{2+} activation with both RLC phosphorylation and dephosphorylation in β-myosin heavy chain isoform (Fig. 6 F). This slowed cross-bridge detachment rate would increase the amount of time cross-bridges bind with actin, potentially contributing to the increased maximum tension observed at longer SLs. This finding differs from that of our prior study, in which RLC phosphorylation slowed cross-bridge detachment at both 1.9- and 2.2-μm SL (Pulcastro et al., 2016). Thus, cross-bridge cycling kinetics were more length dependent in myocardial preparations containing β-myosin heavy chain versus the α-myosin heavy chain isoform (consistent with prior observations in mouse myocardium; Tanner et al., 2014).

We also noted no significant differences in cross-bridge recruitment rates for the β-myosin heavy chain isoform with increases in SL (Fig. 6 D), in contrast with our prior study of the α-myosin heavy chain isoform, in which cross-bridge recruitment rate decreased at 2.2-μm SL. Notably, RLC phosphorylation increased the number of bound cross-bridges at maximal and submaximal Ca^{2+} concentrations for the β-myosin heavy chain isoform (Fig. 6, C and E), which is consistent with our previous findings in α-myosin heavy chain. This consistency suggests that the number of cross-bridges bound is a fundamental mechanism contributing to greater tension development at longer SLs, regardless of the cardiac myosin heavy chain isoform. For the β-myosin heavy chain isoform, we observed increased viscoelastic stiffness at long SL at both submaximal and maximal Ca^{2+} concentration (Fig. 6 A), which was comparable with our findings for the α-myosin heavy chain isoform, but more pronounced in this current study. Together, these data suggest that increased viscoelastic stiffness stems from, or is associated with, greater cross-bridge contributions to length-dependent tension development as SL increases.

Viscous and elastic moduli increased with SL in relaxed strips, but there was no significant change in viscous and elastic moduli with RLC phosphorylation in relaxed strips at either SL. RLC phosphorylation–dependent differences in active moduli occurred only in activated strips. This supports the tension data suggesting that effects of RLC phosphorylation on myosin mechanics are exerted through changes in active contractile processes rather than passive tension. Activated differences in viscous and elastic moduli with RLC phosphorylation were seen only at long SL (Fig. 5), which is consistent with RLC phosphorylation effects on tension (Fig. 3).

Differential myosin heavy chain expression may have functional consequences

β-myosin heavy chain expression correlates negatively with heart rate across various mammal species, with animals of resting heart rates <300 beats per minute predominantly expressing the β-myosin heavy chain isoform in the ventricular myocardium (Hamilton and Ianuzzo, 1991). Thus, relative changes in the speed of molecular processes scale with required speeds to accommodate heart rate, and slower heart rates may allow for more filling time and greater SL dependence to augment power output and larger blood flow volumes in larger animals (Hamilton and Ianuzzo, 1991). Overall, studies have found decreased cross-bridge cycling kinetics in β-myosin heavy chain isoform versus α-myosin heavy chain isoforms (Korte et al., 2005; Rundell et al., 2005). This difference seems to be related to myosin ATPase activity in both isoforms, with α-myosin heavy chain expressing faster myosin ATPase activity and β-myosin heavy chain demonstrating slower ATPase activity (Hamilton and Ianuzzo, 1991). However, these effects are highly length-dependent in β-myosin heavy chain, and the relative length-dependent sensitivity of cross-bridge cycling kinetics is greater for β- versus α-myosin heavy chain in skinned rat myocardial strips (Tanner et al., 2014). In β-myosin heavy chain myocytes, previous studies noted an increase in cross-bridge cycling kinetics at short SL versus long SL that was more closely related to lattice spacing versus tension (Korte and McDonald, 2007). This effect of lattice spacing on cross-bridge cycling was less pronounced in α-myosin heavy chain strips, which were more affected by tension. Moreover, those authors showed greater SL dependence of loaded shortening and peak power output of skinned cardiomyocytes containing β- versus α-myosin heavy chain. In combination with our findings, these data may indicate that the different responsiveness to SL changes between these myosin heavy chain isoforms stems from different sensitivities to myofilament stress or load versus myofilament geometry or lattice spacing. Thus, increased length dependence in β-myosin heavy chain strips may confer functional benefits in human cardiac ventricles (and in hearts of larger mammals), where the operating range of SLs and transmural stress–strain heterogeneities may be greater than those observed for rats or mice (Lewinter et al., 2010). Thus, a greater sensitivity to SL and lattice spacing may result in a steeper Frank–Starling relationship in cardiac tissues predominantly expressing β-myosin heavy chain.

RLC phosphorylation plays a critical role in modulating contractility for both cardiac myosin heavy chain isoforms

We noted that RLC phosphorylation increased tension for both myosin heavy chain isoforms, particularly at long SL (Fig. 3; Pulcastro et al., 2016). This effect may be attributed to smaller thick-to-thin filament spacing as SL increases, sterically promoting cross-bridge binding (Matsubara and Millman, 1974; Granzier and Irving, 1995; Konhilas et al., 2002; Smith et al., 2009). RLC phosphorylation may reposition myosin heads close to the thin filament, further decreasing thick-to-thin filament distance (Colson et al., 2010). Simultaneously, these changes in lattice spacing may provide a physical explanation for decreased cross-bridge detachment rates at longer SLs for both myosin heavy chain isoforms (Fig. 6 F; Pulcastro et al., 2016).

Altogether, these data suggest functional consequences of RLC phosphorylation, regardless of myosin heavy chain isoform expression. Previous studies suggested that RLC phosphorylation may increase myosin stiffness in skeletal muscle (Greenberg et al., 2009). Computational models of cardiac contractility have suggested that RLC phosphorylation enhances twitch force and ventricular torsion throughout a heartbeat (Sheikh et al., 2012) because of increased cross-bridge stiffness (or greater "observed

power-stroke size") as well as faster cross-bridge attachment rates to augment contractility. Combined cross-bridge and twitch mechanics models implementing these multiple mechanisms of RLC phosphorylation were required to recapitulate the measured RLC phosphorylation responses—neither mechanism was sufficient alone (Sheikh et al., 2012). Consistent with these computational predictions, other groups have used single-molecule techniques to measure increases in myosin step size upon RLC phosphorylation for both skeletal and cardiac myosins (Wang et al., 2014), which could contribute to the greater force production that we observed. Our studies measured viscoelastic myocardial stiffness at submaximal and maximal Ca^{2+} concentrations in both myosin heavy chain isoforms (Fig. 5 and Pulcastro et al., 2016). In our study, RLC phosphorylation produced subtle, but statistically significant, increases in myocardial viscoelastic stiffness for myocardial strips expressing β-myosin heavy chain, which could arise from greater numbers of cross-bridges bound (Fig. 6 C) or increases in myosin step-size and stiffness, particularly at 2.2-µm SL (Sheikh et al., 2012; Wang et al., 2014). In contrast, RLC phosphorylation produced slight decreases in viscoelastic myocardial stiffness at both short and long SLs for myocardial strips expressing the α-myosin heavy chain isoform (Pulcastro et al., 2016), suggesting that RLC phosphorylation leads to minimal change or could even decrease α-myosin heavy chain cross-bridge stiffness.

Steric repositioning of the myosin head nearer to thin filaments upon RLC phosphorylation (Levine et al., 1998), along with any potential effects of RLC phosphorylation on cross-bridge stiffness, could combine to alter the strain-dependent or load-dependent kinetics of force-bearing cross-bridges. Increasing SL may independently reduce lattice spacing to diminish cross-bridge strain as well. However, RLC phosphorylation may amplify this effect at long SL to increase myosin step size and slow cross-bridge detachment rate (Fig. 6 F; Wang et al., 2014). This mechanism would be expected to augment force production in both myosin heavy chain isoforms, agreeing with our findings of increased Ca^{2+}-sensitivity of the tension–pCa relationship observed herein and previously (Pulcastro et al., 2016).

RLC phosphorylation and heart disease

At the organ level, the Frank–Starling law of the heart links increased contractility with increased ventricular filling to dynamically accommodate contractile demand on a beat-to-beat basis. Recently, a handful of studies have started to generate a detailed understanding of the intrinsic role that cross-bridge kinetics plays in length-dependent muscle contraction (Adhikari and Wang, 2004; McDonald, 2011; Milani-Nejad et al., 2015; Tanner et al., 2015; Ait-Mou et al., 2016). RLC phosphorylation has been implicated in properly timing contraction to enhance ventricular torsion (Davis et al., 2001; Sheikh et al., 2012), and reductions in RLC phosphorylation accompany cardiac stress and the progression of heart failure (Sanbe et al., 1999; van der Velden et al., 2003; Ding et al., 2010; Sheikh et al., 2012; Warren et al., 2012; Chang et al., 2015). Reduced RLC phosphorylation has also been linked with RLC mutations that cause hypertrophic cardiomyopathy in humans and mice (Szczesna et al., 2001; Abraham et al., 2009; Greenberg et al., 2010; Kazmierczak et al., 2012). Altogether, it is clear that RLC phosphorylation is an important modulator of cardiac function over multiple biological scales, which has motivated a handful of preclinical studies trying to target RLC phosphorylation as a therapeutic mechanism to modulate ventricular function and help prevent the pathological development of cardiomyopathies (Sheikh et al., 2012; Warren et al., 2012; Chang et al., 2015; Yuan et al., 2015).

We showed that the effects of RLC phosphorylation on β-myosin heavy chain contraction are enhanced at longer SLs. As stated previously, SL increases as the ventricle fills, and RLC phosphorylation may help to increase power output from the contracting myocardium to maintain the Frank–Starling law. It is likely that RLC phosphorylation plays an important role in this response, but clearly there are myriad other myofilament proteins that help modulate cross-bridge activity and myocardial contractility throughout a heartbeat. Nonetheless, these data support the idea that a basal level of RLC phosphorylation would benefit normal cardiac function (Chang et al., 2016), and dysregulation or decreases in RLC phosphorylation might then lead to signaling for hypertrophic compensation, ultimately manifesting as hypertrophic cardiomyopathy. Better understanding this mechanism may be a key to understanding the pathogenesis of severe forms of hypertrophic cardiomyopathy with sudden cardiac death.

Potential effects of PTU-induced hypothyroidism

Passive tension is predominantly caused by titin at shorter SLs and collagen at longer SLs (Granzier and Irving, 1995). PTU-induced hypothyroidism has been shown to induce myofibril and myofilament disorganization, disruption, and rupture; increase interstitial substance; and reduce fiber mass (Lopes et al., 1993; Massoud et al., 2012). To explore the effects this might have on passive tension, we performed a *t* test comparing our PTU-treated measurements to those in a previous study from our laboratory (Pulcastro et al., 2016). Between the two studies, passive tension decreased in PTU-treated strips at 1.9-µm SL; from 0.72 to 0.39 $kN \cdot m^{-2}$ for AP-treated strips ($P = 0.0001$) and from 0.54 to 0.39 $kN \cdot m^{-2}$ for MLCK-treated strips ($P = 0.0001$). When comparing similar passive tension measurements at 2.2-µm SL between the two studies, we found no significant effects of PTU, irrespective of AP or MLCK treatment. We suspect that any myofibril disruption from PTU would contribute to less passive tension at the 1.9-µm SL, because titin is an integral part of the sarcomere. Primary hypothyroidism has been shown to increase interstitial collagen deposition in rat myocardium (Drobnik et al., 2009), which we would expect to increase passive tension at longer SLs in PTU-treated strips that is related to increased collagen deposition, but this was not the case. Thus, there may be some subtle myofibrillar or ultrastructural differences caused by PTU treatment that have a small effect on length-dependent passive tension development.

Apart from any potential structural differences, decreased passive tension values could follow from changes in titin isoform expression elicited by PTU treatment. Hypothyroidism may lead to alternative splicing or signaling that switches titin isoform expression from the adult N2B titin isoform to the more compliant fetal N2BA titin isoform (Wu et al., 2007; Krüger et al., 2008). Further study of this isoform in bovine myocardium showed that greater expression of N2BA titin blunted length-dependent ten-

sion development and Ca^{2+} sensitivity of contraction (Fukuda et al., 2005). Thus, we might have expected our observed effects of SL to be blunted by a similar switch in titin isoform expression, rather than enhanced effects of SL and RLC phosphorylation at long SLs that we measured herein. One important note is that these length-dependent changes from titin isoform switching required preincubation in protein kinase A (Yamasaki et al., 2002; Fukuda et al., 2005).

SR calcium ATPase (SERCA2), β-adrenergic receptors, sodium/potassium ATPases, and several potassium channels ($K_v1.5$, $K_v4.2$, and $K_v4.3$) have been shown to be affected by hypothyroidism (Hajje et al., 2014). Although these proteins are necessary for cardiac function, we controlled Ca^{2+} activation and electrolyte concentrations in our solutions. Therefore, although hypothyroidism may induce cardiac dysfunction, any differences we would expect to see in our preparations may solely underlie the differences in passive tension discussed at the beginning of this section and should not affect our results regarding active tension development and cross-bridge kinetics. Furthermore, any structural changes would have been present in all of our fibers, but our results showed changes in contractility only at longer SL associated with MLCK incubation. Altogether, these findings and potential limitations imply that the changes in active tension development and Ca^{2+} sensitivity that we observed stem from length-dependent effects of MLCK treatment and increased RLC phosphorylation, rather than aberrant artifacts of PTU treatment.

In the present study, we developed an understanding of the interaction of β-myosin heavy chain and RLC, two proteins implicated in the development of heart failure and particularly hypertrophic cardiomyopathy. Heavy accumulation of extracellular matrix and increased myocardial stiffness are hallmarks of hypertrophied and failing hearts (Biernacka and Frangogiannis, 2011; Wong et al., 2012; Venkatesh et al., 2014; Wong, 2014). Although we have outlined potential hypothyroid-induced changes in the myocardium, we believe these changes do not influence our overall conclusions, but acknowledge that they may also contribute to fibrotic cardiac remodeling associated with hypertrophic cardiomyopathy and the progression of heart failure (none of which were readily observable in the PTU-treated rat hearts used in this study).

Acknowledgments

These studies were supported by an American Heart Association grant (17SDG33370153) and a National Science Foundation grant (1656450).

The authors declare no competing financial interests.

Author contributions: P.O. Awinda and B.C.W. Tanner conceived the study and designed the experiments. All authors were involved in data acquisition, data analysis, and data interpretation. J.J. Breithaupt, H.C. Pulcastro, and B.C.W. Tanner drafted the manuscript. All authors contributed to reviewing, editing, and approving the final version of the manuscript.

Henk L. Granzier served as editor.

Submitted: 18 June 2018
Accepted: 7 November 2018

References

Abraham, T.P., M. Jones, K. Kazmierczak, H.-Y. Liang, A.C. Pinheiro, C.S. Wagg, G.D. Lopaschuk, and D. Szczesna-Cordary. 2009. Diastolic dysfunction in familial hypertrophic cardiomyopathy transgenic model mice. *Cardiovasc. Res.* 82:84–92. https://doi.org/10.1093/cvr/cvp016

Adhikari, B.B., and K. Wang. 2004. Interplay of troponin- and myosin-based pathways of calcium activation in skeletal and cardiac muscle: The use of W7 as an inhibitor of thin filament activation. *Biophys. J.* 86:359–370. https://doi.org/10.1016/S0006-3495(04)74112-0

Ait-Mou, Y., K. Hsu, G.P. Farman, M. Kumar, M.L. Greaser, T.C. Irving, and P.P. de Tombe. 2016. Titin strain contributes to the Frank-Starling law of the heart by structural rearrangements of both thin- and thick-filament proteins. *Proc. Natl. Acad. Sci. USA.* 113:2306–2311. https://doi.org/10.1073/pnas.1516732113

Biernacka, A., and N.G. Frangogiannis. 2011. Aging and cardiac fibrosis. *Aging Dis.* 2:158–173. https://doi.org/10.1016/j.bbi.2008.05.010

Campbell, K.B., M. Chandra, R.D. Kirkpatrick, B.K. Slinker, and W.C. Hunter. 2004. Interpreting cardiac muscle force-length dynamics using a novel functional model. *Am. J. Physiol. Heart Circ. Physiol.* 286:H1535–H1545. https://doi.org/10.1152/ajpheart.01029.2003

Chang, A.N., P.K. Battiprolu, P.M. Cowley, G. Chen, R.D. Gerard, J.R. Pinto, J.A. Hill, A.J. Baker, K.E. Kamm, and J.T. Stull. 2015. Constitutive phosphorylation of cardiac myosin regulatory light chain in vivo. *J. Biol. Chem.* 290:10703–10716. https://doi.org/10.1074/jbc.M115.642165

Chang, A.N., K.E. Kamm, and J.T. Stull. 2016. Role of myosin light chain phosphatase in cardiac physiology and pathophysiology. *J. Mol. Cell. Cardiol.* 101:35–43. https://doi.org/10.1016/j.yjmcc.2016.10.004

Colson, B.A., M.R. Locher, T. Bekyarova, J.R. Patel, D.P. Fitzsimons, T.C. Irving, and R.L. Moss. 2010. Differential roles of regulatory light chain and myosin binding protein-C phosphorylations in the modulation of cardiac force development. *J. Physiol.* 588:981–993. https://doi.org/10.1113/jphysiol.2009.183897

Cooke, R. 1997. Actomyosin interaction in striated muscle. *Physiol. Rev.* 77:671–697. https://doi.org/10.1152/physrev.1997.77.3.671

Davis, J.S., S. Hassanzadeh, S. Winitsky, H. Lin, C. Satorius, R. Vemuri, A.H. Aletras, H. Wen, and N.D. Epstein. 2001. The overall pattern of cardiac contraction depends on a spatial gradient of myosin regulatory light chain phosphorylation. *Cell.* 107:631–641. https://doi.org/10.1016/S0092-8674(01)00586-4

Ding, P., J. Huang, P.K. Battiprolu, J.A. Hill, K.E. Kamm, and J.T. Stull. 2010. Cardiac myosin light chain kinase is necessary for myosin regulatory light chain phosphorylation and cardiac performance in vivo. *J. Biol. Chem.* 285:40819–40829. https://doi.org/10.1074/jbc.M110.160499

Drobnik, J., J. Ciosek, D. Slotwinska, B. Stempniak, D. Zukowska, A. Marczynski, D. Tosik, H. Bartel, R. Dabrowski, and A. Szczepanowska. 2009. Experimental hypothyroidism increases content of collagen and glycosaminoglycans in the heart. *J. Physiol. Pharmacol.* 60:57–62.

Fitzsimons, D.P., J.R. Patel, and R.L. Moss. 1998. Role of myosin heavy chain composition in kinetics of force development and relaxation in rat myocardium. *J. Physiol.* 513:171–183.

Ford, S.J., and M. Chandra. 2013. Length-dependent effects on cardiac contractile dynamics are different in cardiac muscle containing α- or β-myosin heavy chain. *Arch. Biochem. Biophys.* 535:3–13. https://doi.org/10.1016/j.abb.2012.10.011

Franks, K., R. Cooke, and J.T. Stull. 1984. Myosin phosphorylation decreases the ATPase activity of cardiac myofibrils. *J. Mol. Cell. Cardiol.* 16:597–604. https://doi.org/10.1016/S0022-2828(84)80624-0

Fukuda, N., Y. Wu, P. Nair, and H.L. Granzier. 2005. Phosphorylation of titin modulates passive stiffness of cardiac muscle in a titin isoform-dependent manner. *J. Gen. Physiol.* 125:257–271. https://doi.org/10.1085/jgp.200409177

Godt, R.E., and B.D. Lindley. 1982. Influence of temperature upon contractile activation and isometric force production in mechanically skinned muscle fibers of the frog. *J. Gen. Physiol.* 80:279–297. https://doi.org/10.1085/jgp.80.2.279

Granzier, H.L., and T.C. Irving. 1995. Passive tension in cardiac muscle: contribution of collagen, titin, microtubules, and intermediate filaments. *Biophys. J.* 68:1027–1044. https://doi.org/10.1016/S0006-3495(95)80278-X

Greenberg, M.J., T.R. Mealy, J.D. Watt, M. Jones, D. Szczesna-Cordary, and J.R. Moore. 2009. The molecular effects of skeletal muscle myosin regulatory light chain phosphorylation. *Am. J. Physiol. Regul. Integr. Comp. Physiol.* 297:R265–R274. https://doi.org/10.1152/ajpregu.00171.2009

Greenberg, M.J., K. Kazmierczak, D. Szczesna-Cordary, and J.R. Moore. 2010. Cardiomyopathy-linked myosin regulatory light chain mutations dis-

rupt myosin strain-dependent biochemistry. *Proc. Natl. Acad. Sci. USA.* 107:17403–17408. https://doi.org/10.1073/pnas.1009619107

Hajje, G., Y. Saliba, T. Itani, M. Moubarak, G. Aftimos, and N. Farès. 2014. Hypothyroidism and its rapid correction alter cardiac remodeling. *PLoS One.* 9:e109753. https://doi.org/10.1371/journal.pone.0109753

Hamilton, N., and C.D. Ianuzzo. 1991. Contractile and calcium regulating capacities of myocardia of different sized mammals scale with resting heart rate. *Mol. Cell. Biochem.* 106:133–141. https://doi.org/10.1007/BF00230179

Kawai, M., and H.R. Halvorson. 1991. Two step mechanism of phosphate release and the mechanism of force generation in chemically skinned fibers of rabbit psoas muscle. *Biophys. J.* 59:329–342. https://doi.org/10.1016/S0006-3495(91)82227-5

Kazmierczak, K., P. Muthu, W. Huang, M. Jones, Y. Wang, and D. Szczesna-Cordary. 2012. Myosin regulatory light chain mutation found in hypertrophic cardiomyopathy patients increases isometric force production in transgenic mice. *Biochem. J.* 442:95–103. https://doi.org/10.1042/BJ20111145

Konhilas, J.P., T.C. Irving, and P.P. de Tombe. 2002. Myofilament calcium sensitivity in skinned rat cardiac trabeculae: role of interfilament spacing. *Circ. Res.* 90:59–65. https://doi.org/10.1161/hh0102.102269

Korte, F.S., and K.S. McDonald. 2007. Sarcomere length dependence of rat skinned cardiac myocyte mechanical properties: dependence on myosin heavy chain. *J. Physiol.* 581:725–739. https://doi.org/10.1113/jphysiol.2007.128199

Korte, F.S., T.J. Herron, M.J. Rovetto, and K.S. McDonald. 2005. Power output is linearly related to MyHC content in rat skinned myocytes and isolated working hearts. *Am. J. Physiol. Heart Circ. Physiol.* 289:H801–H812. https://doi.org/10.1152/ajpheart.01227.2004

Krüger, M., C. Sachse, W.H. Zimmermann, T. Eschenhagen, S. Klede, and W.A. Linke. 2008. Thyroid hormone regulates developmental titin isoform transitions via the phosphatidylinositol-3-kinase/AKT pathway. *Circ. Res.* 102:439–447. https://doi.org/10.1161/CIRCRESAHA.107.162719

Levine, R.J.C., Z. Yang, N.D. Epstein, L. Fananapazir, J.T. Stull, and H.L. Sweeney. 1998. Structural and functional responses of mammalian thick filaments to alterations in myosin regulatory light chains. *J. Struct. Biol.* 122:149–161. https://doi.org/10.1006/jsbi.1998.3980

Lewinter, M.M., J. Popper, M. McNabb, L. Nyland, S.B. Bell, and H. Granzier. 2010. Extensible behavior of titin in the miniswine left ventricle. *Circulation.* 121:768–774. https://doi.org/10.1161/CIRCULATIONAHA.109.918151

Lompré, A.M., B. Nadal-Ginard, and V. Mahdavi. 1984. Expression of the cardiac ventricular alpha- and beta-myosin heavy chain genes is developmentally and hormonally regulated. *J. Biol. Chem.* 259:6437–6446.

Lopes, A.C., R. Furlanetto, W.S. Sasso, and L.J. Didio. 1993. Subcellular alterations of cardiac fibers in rats subjected to hypothyroidism. *J. Submicrosc. Cytol. Pathol.* 25:263–266.

Massoud, A.A., A. El-Atrash, E. Tousson, W. Ibrahim, and H. Abou-Harga. 2012. Light and ultrastructural study in the propylthiouracil-induced hypothyroid rat heart ventricles and the ameliorating role of folic acid. *Toxicol. Ind. Health.* 28:262–270. https://doi.org/10.1177/0748233711410915

Matsubara, I., and B.M. Millman. 1974. X-ray diffraction patterns from mammalian heart muscle. *J. Mol. Biol.* 82:527–536. https://doi.org/10.1016/0022-2836(74)90246-0

McDonald, K.S. 2011. The interdependence of Ca2+ activation, sarcomere length, and power output in the heart. *Pflugers Arch.* 462:61–67. https://doi.org/10.1007/s00424-011-0949-y

Milani-Nejad, N., B.D. Canan, M.T. Elnakish, J.P. Davis, J.-H. Chung, V.V. Fedorov, P.F. Binkley, R.S.D. Higgins, A. Kilic, P.J. Mohler, and P.M.L. Janssen. 2015. The Frank-Starling mechanism involves deceleration of cross-bridge kinetics and is preserved in failing human right ventricular myocardium. *Am. J. Physiol. Heart Circ. Physiol.* 309:H2077–H2086. https://doi.org/10.1152/ajpheart.00685.2015

Morano, I., F. Hofmann, M. Zimmer, and J.C. Rüegg. 1985. The influence of P-light chain phosphorylation by myosin light chain kinase on the calcium sensitivity of chemically skinned heart fibres. *FEBS Lett.* 189:221–224. https://doi.org/10.1016/0014-5793(85)81027-9

Mulieri, L.A., W. Barnes, B.J. Leavitt, F.P. Ittleman, M.M. LeWinter, N.R. Alpert, and D.W. Maughan. 2002. Alterations of myocardial dynamic stiffness implicating abnormal crossbridge function in human mitral regurgitation heart failure. *Circ. Res.* 90:66–72. https://doi.org/10.1161/hh0102.103221

Olsson, M.C., J.R. Patel, D.P. Fitzsimons, J.W. Walker, and R.L. Moss. 2004. Basal myosin light chain phosphorylation is a determinant of Ca2+ sensitivity of force and activation dependence of the kinetics of myocardial force development. *Am. J. Physiol. Heart Circ. Physiol.* 287:H2712–H2718. https://doi.org/10.1152/ajpheart.01067.2003

Palmer, B.M. 2010. A strain-dependency of myosin off-rate must be sensitive to frequency to predict the B-process of sinusoidal analysis. *Adv. Exp. Med. Biol.* 682:57–75. https://doi.org/10.1007/978-1-4419-6366-6_4

Palmer, B.M., T. Suzuki, Y. Wang, W.D. Barnes, M.S. Miller, and D.W. Maughan. 2007. Two-state model of acto-myosin attachment-detachment predicts C-process of sinusoidal analysis. *Biophys. J.* 93:760–769. https://doi.org/10.1529/biophysj.106.101626

Palmer, B.M., J.P. Schmitt, C.E. Seidman, J.G. Seidman, Y. Wang, S.P. Bell, M.M. Lewinter, and D.W. Maughan. 2013. Elevated rates of force development and MgATP binding in F764L and S532P myosin mutations causing dilated cardiomyopathy. *J. Mol. Cell. Cardiol.* 57:23–31. https://doi.org/10.1016/j.yjmcc.2012.12.022

Patel, J.R., G.M. Diffee, X.P. Huang, and R.L. Moss. 1998. Phosphorylation of myosin regulatory light chain eliminates force-dependent changes in relaxation rates in skeletal muscle. *Biophys. J.* 74:360–368. https://doi.org/10.1016/S0006-3495(98)77793-8

Pope, B., J.F.Y. Hoh, and A. Weeds. 1980. The ATPase activities of rat cardiac myosin isoenzymes. *FEBS Lett.* 118:205–208. https://doi.org/10.1016/0014-5793(80)80219-5

Pulcastro, H.C., P.O. Awinda, J.J. Breithaupt, and B.C.W. Tanner. 2016. Effects of myosin light chain phosphorylation on length-dependent myosin kinetics in skinned rat myocardium. *Arch. Biochem. Biophys.* 601:56–68. https://doi.org/10.1016/j.abb.2015.12.014

Reiser, P.J., and W.O. Kline. 1998. Electrophoretic separation and quantitation of cardiac myosin heavy chain isoforms in eight mammalian species. *Am. J. Physiol.* 274:H1048–H1053.

Reiser, P.J., M.A. Portman, X.H. Ning, and C. Schomisch Moravec. 2001. Human cardiac myosin heavy chain isoforms in fetal and failing adult atria and ventricles. *Am. J. Physiol. Heart Circ. Physiol.* 280:H1814–H1820. https://doi.org/10.1152/ajpheart.2001.280.4.H1814

Rundell, V.L.M., V. Manaves, A.F. Martin, and P.P. de Tombe. 2005. Impact of beta-myosin heavy chain isoform expression on cross-bridge cycling kinetics. *Am. J. Physiol. Heart Circ. Physiol.* 288:H896–H903. https://doi.org/10.1152/ajpheart.00407.2004

Sanbe, A., J.G. Fewell, J. Gulick, H. Osinska, J. Lorenz, D.G. Hall, L.A. Murray, T.R. Kimball, S.A. Witt, and J. Robbins. 1999. Abnormal cardiac structure and function in mice expressing nonphosphorylatable cardiac regulatory myosin light chain 2. *J. Biol. Chem.* 274:21085–21094. https://doi.org/10.1074/jbc.274.30.21085

Sheikh, F., K. Ouyang, S.G. Campbell, R.C. Lyon, J. Chuang, D. Fitzsimons, J. Tangney, C.G. Hidalgo, C.S. Chung, H. Cheng, et al. 2012. Mouse and computational models link Mlc2v dephosphorylation to altered myosin kinetics in early cardiac disease. *J. Clin. Invest.* 122:1209–1221. https://doi.org/10.1172/JCI61134

Smith, L., C. Tainter, M. Regnier, and D.A. Martyn. 2009. Cooperative cross-bridge activation of thin filaments contributes to the Frank-Starling mechanism in cardiac muscle. *Biophys. J.* 96:3692–3702. https://doi.org/10.1016/j.bpj.2009.02.018

Stelzer, J.E., J.R. Patel, and R.L. Moss. 2006. Acceleration of stretch activation in murine myocardium due to phosphorylation of myosin regulatory light chain. *J. Gen. Physiol.* 128:261–272. https://doi.org/10.1085/jgp.200609547

Sweeney, H.L., and J.T. Stull. 1986. Phosphorylation of myosin in permeabilized mammalian cardiac and skeletal muscle cells. *Am. J. Physiol.* 250:C657–C660. https://doi.org/10.1152/ajpcell.1986.250.4.C657

Sweeney, H.L., and J.T. Stull. 1990. Alteration of cross-bridge kinetics by myosin light chain phosphorylation in rabbit skeletal muscle: implications for regulation of actin-myosin interaction. *Proc. Natl. Acad. Sci. USA.* 87:414–418. https://doi.org/10.1073/pnas.87.1.414

Sweeney, H.L., B.F. Bowman, and J.T. Stull. 1993. Myosin light chain phosphorylation in vertebrate striated muscle: regulation and function. *Am. J. Physiol.* 264:C1085–C1095. https://doi.org/10.1152/ajpcell.1993.264.5.C1085

Szczesna, D., D. Ghosh, Q. Li, A.V. Gomes, G. Guzman, C. Arana, G. Zhi, J.T. Stull, and J.D. Potter. 2001. Familial hypertrophic cardiomyopathy mutations in the regulatory light chains of myosin affect their structure, Ca2+ binding, and phosphorylation. *J. Biol. Chem.* 276:7086–7092. https://doi.org/10.1074/jbc.M009823200

Tanner, B.C.W., Y. Wang, D.W. Maughan, and B.M. Palmer. 2011. Measuring myosin cross-bridge attachment time in activated muscle fibers using stochastic vs. sinusoidal length perturbation analysis. *J. Appl. Physiol.* 110:1101–1108. https://doi.org/10.1152/japplphysiol.00800.2010

Tanner, B.C.W., Y. Wang, J. Robbins, and B.M. Palmer. 2014. Kinetics of cardiac myosin isoforms in mouse myocardium are affected differently by presence of myosin binding protein-C. *J. Muscle Res. Cell Motil.* 35:267–278. https://doi.org/10.1007/s10974-014-9390-0

Tanner, B.C.W., J.J. Breithaupt, and P.O. Awinda. 2015. Myosin MgADP release rate decreases at longer sarcomere length to prolong myosin attachment time in skinned rat myocardium. *Am. J. Physiol. Heart Circ. Physiol.* 309:H2087–H2097. https://doi.org/10.1152/ajpheart.00555.2015

Tobacman, L.S. 1996. Thin filament-mediated regulation of cardiac contraction. *Annu. Rev. Physiol.* 58:447–481. https://doi.org/10.1146/annurev.ph.58.030196.002311

van der Velden, J., Z. Papp, N.M. Boontje, R. Zaremba, J.W. de Jong, P.M. Janssen, G. Hasenfuss, and G.J. Stienen. 2003. The effect of myosin light chain 2 dephosphorylation on Ca2+ sensitivity of force is enhanced in failing human hearts. *Cardiovasc. Res.* 57:505–514. https://doi.org/10.1016/S0008-6363(02)00662-4

Venkatesh, B.A., G.J. Volpe, S. Donekal, N. Mewton, C.Y. Liu, S.J. Shea, K. Liu, G. Burke, C. Wu, D.A. Bluemke, and J.A.C. Lima. 2014. Association of longitudinal changes in left ventricular structure and function with myocardial fibrosis: The MESA study RR. *Hypertension.* 64:508–515. https://doi.org/10.1161/HYPERTENSIONAHA.114.03697

Wang, Y., B.C.W. Tanner, A.T. Lombardo, S.M. Tremble, D.W. Maughan, P. Vanburen, M.M. Lewinter, J. Robbins, and B.M. Palmer. 2013. Cardiac myosin isoforms exhibit differential rates of MgADP release and MgATP binding detected by myocardial viscoelasticity. *J. Mol. Cell. Cardiol.* 54:1–8. https://doi.org/10.1016/j.yjmcc.2012.10.010

Wang, Y., K. Ajtai, and T.P. Burghardt. 2014. Ventricular myosin modifies in vitro step-size when phosphorylated. *J. Mol. Cell. Cardiol.* 72:231–237. https://doi.org/10.1016/j.yjmcc.2014.03.022

Warren, S.A., L.E. Briggs, H. Zeng, J. Chuang, E.I. Chang, R. Terada, M. Li, M.S. Swanson, S.H. Lecker, M.S. Willis, et al. 2012. Myosin light chain phosphorylation is critical for adaptation to cardiac stress. *Circulation.* 126:2575–2588. https://doi.org/10.1161/CIRCULATIONAHA.112.116202

Wong, T.C. 2014. Cardiovascular magnetic resonance imaging of myocardial interstitial expansion in hypertrophic cardiomyopathy. *Curr. Cardiovasc. Imaging Rep.* 7:9267. https://doi.org/10.1007/s12410-014-9267-z

Wong, T.C., K. Piehler, C.G. Meier, S.M. Testa, A.M. Klock, A.A. Aneizi, J. Shakesprere, P. Kellman, S.G. Shroff, D.S. Schwartzman, et al. 2012. Association between extracellular matrix expansion quantified by cardiovascular magnetic resonance and short-term mortality. *Circulation.* 126:1206–1216. https://doi.org/10.1161/CIRCULATIONAHA.111.089409

Wu, Y., J. Peng, K.B. Campbell, S. Labeit, and H. Granzier. 2007. Hypothyroidism leads to increased collagen-based stiffness and re-expression of large cardiac titin isoforms with high compliance. *J. Mol. Cell. Cardiol.* 42:186–195. https://doi.org/10.1016/j.yjmcc.2006.09.017

Yamasaki, R., Y. Wu, M. McNabb, M. Greaser, S. Labeit, and H. Granzier. 2002. Protein kinase A phosphorylates titin's cardiac-specific N2B domain and reduces passive tension in rat cardiac myocytes. *Circ. Res.* 90:1181–1188. https://doi.org/10.1161/01.RES.0000021115.24712.99

Yuan, C.-C., P. Muthu, K. Kazmierczak, J. Liang, W. Huang, T.C. Irving, R.M. Kanashiro-Takeuchi, J.M. Hare, and D. Szczesna-Cordary. 2015. Constitutive phosphorylation of cardiac myosin regulatory light chain prevents development of hypertrophic cardiomyopathy in mice. *Proc. Natl. Acad. Sci. USA.* 112:E4138–E4146. https://doi.org/10.1073/pnas.1505819112